Chinese Journal of
POLYMER SCIENCE

RESEARCH ARTICLE

https://doi.org/10.1007/s10118-024-3192-7
Chinese J. Polym. Sci. **2024**, *42*, 1442–1448

Regulating Actuations and Shapes of Liquid Crystal Elastomers through Combining Dynamic Covalent Bonds with Cooling-Rate-Mediated Control

Ya-Wen Liu[a,†], Huan Liang[a,†*], Hong-Tu Xu[a], En-Jian He[a], Zhi-Jun Yang[a], Yi-Xuan Wang[a], Yen Wei[a], Zhen Li[b*], and Yan Ji[a*]

[a] *The Key Laboratory of Bioorganic Phosphorus Chemistry & Chemical Biology (Ministry of Education), Department of Chemistry, Tsinghua University, Beijing 100084, China*
[b] *Advanced Materials and Energy Center, Academy of Aerospace Science and Innovation, Beijing 100088, China*

Electronic Supplementary Information

Abstract Realizing multiple locked shapes in pre-oriented liquid crystal elastomers (LCEs) is highly desired for diversifying deformations and enhancing multi-functionality. However, conventional LCEs only deform between two shapes for each actuation cycle upon liquid crystal-isotropic phase transitions induced by external stimuli. Here, we propose to regulate the actuation modes and the locked shapes of a pre-orientated epoxy LCE by combining dynamic covalent bonds with cooling-rate-mediated control. The actuation modes can be adjusted on demand by exchange reactions of dynamic covalent bonds. Derived from the established actuation modes, such as elongation, bending, and spiraling, the epoxy LCE displays varied locked shapes at room temperature under different cooling rates. Various mediums are utilized to control the cooling rate, including water, silicone oil, and copper plates. This approach provides a novel way for regulating the actuation modes and locked shapes of cutting-edge intelligent devices.

Keywords Liquid crystal elastomer; Epoxy; Dynamic covalent bond; Vitrimer; Cooling rate

Citation: Liu, Y. W.; Liang, H.; Xu, H. T.; He, E. J.; Yang, Z. J.; Wang, Y. X.; Wei, Y.; Li, Z.; Ji, Y. Regulating actuations and shapes of liquid crystal elastomers through combining dynamic covalent bonds with cooling-rate-mediated control. *Chinese J. Polym. Sci.* **2024**, *42*, 1442–1448.

INTRODUCTION

Liquid crystal elastomers (LCEs) can undergo large and reversible deformations under external stimuli, which promise them broad application prospects in the fields of artificial muscles, aerospace, biomedical devices, damping devices, *etc*.[1–5] After orientation, LCEs show reversible actuations upon the liquid crystal-isotropic phase transition.[6–8] However, most LCEs only exhibit reversible deformation between two permanent shapes in an actuation cycle. Introducing multiple locked shapes on a single pre-oriented monodomain LCE sample is highly demanded for intelligent shape-shifting systems.[9,10] Several methods have been developed for regulating locked shapes of pre-orientated LCEs. For instance, the design of combining crystalline melting transition and liquid crystal transition into the network structure design enables LCEs with multi-stage shape memory.[11] In addition, bidirectional actuation behaviors (triple-locked shapes) can be realized in dielectric LCEs by changing the electric field direction.[12] Moreover, by utilizing the supercritical behavior of LCEs, precisely controllable locked shapes can be achieved under different temperatures.[13] Despite the advances, these methods generally require continuous external stimuli or energy input (such as heating or electric field) to maintain multiple locked shapes.

For LCEs with predetermined actuation modes, it is a straightforward and convenient method to modulate their locked shapes at room temperature by adjusting cooling rates.[14,15] Since LCEs undergo a first-order isotropic to nematic transition and are sensitive to temperature change rates, heating oriented LCEs to an isotropic state and subsequently cooling them to room temperature by different cooling rates can result in variations in the obtained locked shapes.[16–18] It should be noted that the maintenance of locked shapes does not require any external supply. Furthermore, using this cooling-rate-mediated strategy, the locked shapes at room temperature can be flexibly adjusted by repeatedly heating and then cooling with another cooling rate. Despite the advantages mentioned above, to date, only iso-

* Corresponding authors, E-mail: lianghuan@mail.tsinghua.edu.cn (H.L.)
E-mail: lizhen_casi@163.com (Z.L.)
E-mail: jiyan@tsinghua.edu.cn (Y.J.)
† These authors contributed equally to this work.
Special Issue: Dynamic Polymer Networks
Received April 25, 2024; Accepted June 12, 2024; Published online August 27, 2024

lated cases have been reported involving this strategy. One case combines LCE film and shape memory polymer film to fabricate bilayer actuators, and utilizes varying cooling rates to achieve different locked shapes.[15] However, the actuation modes of these actuators were limited to bending and its derived motions, due to the different deformation ratios between two layers. The other case is based on a type of LCE with low glass transition temperature (T_g, about −6.4 °C).[14] Although the shapes can be regulated, the low T_g can lead to the potential risk of poor stability for a prolonged time at room temperature. Moreover, the locked shapes in the above two cases do not involve reprogramming the actuation modes of LCEs.

The introduction of dynamic covalent bonds into LCEs for orientation and reprogramming of actuation modes has attracted much attention over the past ten years.[19–21] Crosslinked polymers with dynamic covalent bonds are covalent adaptable networks (CANs).[22–24] They can rearrange their topological structures by the reversible reaction of dynamic covalent bonds.[25] CANs that involve exchange reactions and maintain network integrity during reprocessing are vitrimers.[26,27] Their characteristic reprogramming temperature is topology freezing transition temperature (T_v).[28–30] By heating exchangeable LCEs (xLCEs) above the T_v along with applying external force, the xLCEs can be permanently oriented *via* network rearrangement. Using the same method, the actuation modes can be reprogrammed through reprocessing pre-orientation patterns.

Here, we propose to regulate the actuation modes and locked shapes of xLCEs by combining dynamic covalent bonds with cooling-rate-mediated control. An epoxy xLCE with a T_g higher than room temperature is chosen for stable shape locking. Owing to the transesterification, the epoxy LCE can be orientated and tailored to obtain desired actuation modes. In addition, the exchange reaction allows for reprogramming other actuation modes. Based on the predetermined actuation modes, obtained locked shapes at room temperature vary by heating the oriented LCE above the isotropic transition temperature (T_i) and subsequently cooling it down to room temperature under different cooling rates. Diverse locked shapes are demonstrated, which derive from elongating, bending, and spiraling modes. Moreover, different mediums are applied to control cooling rates, including water, silicone oil, and copper plates.

EXPERIMENTAL

General Considerations

Phenol (99%), chloroacetone (98%) and epichlorohydrin (99%) were purchased from J&K Scientific. Triazobicyclodecene (TBD, 98%) and sebacic acid (99%) were purchased from TCI Shanghai. Dichloromethane (DCM), ethanol, isopropyl alcohol, sulfuric acid and sodium hydroxide was purchased from Beijing Tong Guang Fine Chemicals Company. All the chemicals above were used directly without further purification. 4,4′-Dihydroxy-*α*-methylstilbene (DHMS) and diglycidyl ether of 4,4′-dihydroxy-*α*-methylstibene (DGE-DHMS) were synthesized following the procedure outlined in previous works.[31] Specific chemical synthesis equations of DHMS and DGE-DHMS were shown in Fig. S1 (in the electronic supplementary information, ESI). From the ^{1}H-NMR spectra (Fig. S2 in ESI), the specific signals of DGE-DHMS can be clearly identified.

Synthesis of the Polydomain xLCE

The preparation of the xLCE was similar to the procedure described in our previous work.[32] As shown in Fig. 1(a), stoichiometric amounts of DGE-DHMS and sebacic acid were mixed at 160 °C. The TBD catalyst (1 mol% to the COOH groups) was introduced and stirred manually until the mixture was too viscous to flow. Subsequently, the mixture was cooled to room temperature and transferred into a custom-developed mold prepared by combining two pieces of PTFE films with a spacer of the desired thickness. The whole set was cured at 160 °C for 6 h under a pressure of 4 MPa using a hot press, and then the polydomain xLCE film was obtained. The specific cross-linking structure of the xLCE was shown in Fig. 1(b).

Synthesis of the Monodomain xLCE

To obtain a monodomain xLCE, the as-prepared polydomain xLCE film was uniaxially stretched to 30% strain, and the deformation was fixed by PTFE tapes on a glass slide. Alignment was established *via* dynamic transesterification after keeping the film at 160 °C for 2 h using a heating stage. Subsequently, the cooled film was taken off and annealed at 100 °C to acquire a monodomain xLCE.

Synthesis of xLCEs with Different Actuation Modes

The reversible elongation actuation mode was obtained by stretching the xLCE film uniaxially to 30% strain and fixing it with Teflon tapes. The fixed film was heated at 160 °C for 2 h to allow dynamic reactions to occur. After annealing at 100 °C, the monodomain xLCE with reversible elongation actuation mode was acquired.

The reversible bending actuation mode was obtained by coating the black ink on the surface of the monodomain xLCE to form a bilayer structure. Owing to the constraints of the rigid black ink layer (passive layer), the actuator exhibited bending actuation upon heating.

The reversible spiraling actuation mode was achieved by reprogramming the monodomain xLCE with elongation actuation mode. The xLCE film was winded around a Teflon tube for several circles and fixed by Teflon tapes. The following procedures were the same as those used in preparing the xLCE with elongation motion.

RESULTS AND DISCUSSION

Swelling experiments of the xLCE were conducted and the gel fraction was 97%, indicating sufficient cross-linking in the xLCE (Fig. S3 in ESI). Fourier transform infrared (FTIR) spectra show that epoxy groups (912 cm^{-1}) are totally converted, indicating the xLCE materials were fully cross-linked (Fig. 1c and Fig. S4 in ESI). According to the differential scanning calorimetry (DSC) curve of the xLCE, the glass transition temperature (T_g) and the isotropic transition temperature (T_i) were approximately 34 and 78 °C, respectively (Fig. 1d). In addition, the thermal stabilities of the sample were characterized by thermogravimetric analysis (TGA, Fig. S5 in ESI). The decomposition temperature (T_d), *i.e.*, the onset of decomposition (1% weight loss) for the samples under an air and nitrogen atmosphere was about 262 and 271 °C, respectively.

https://doi.org/10.1007/s10118-024-3192-7

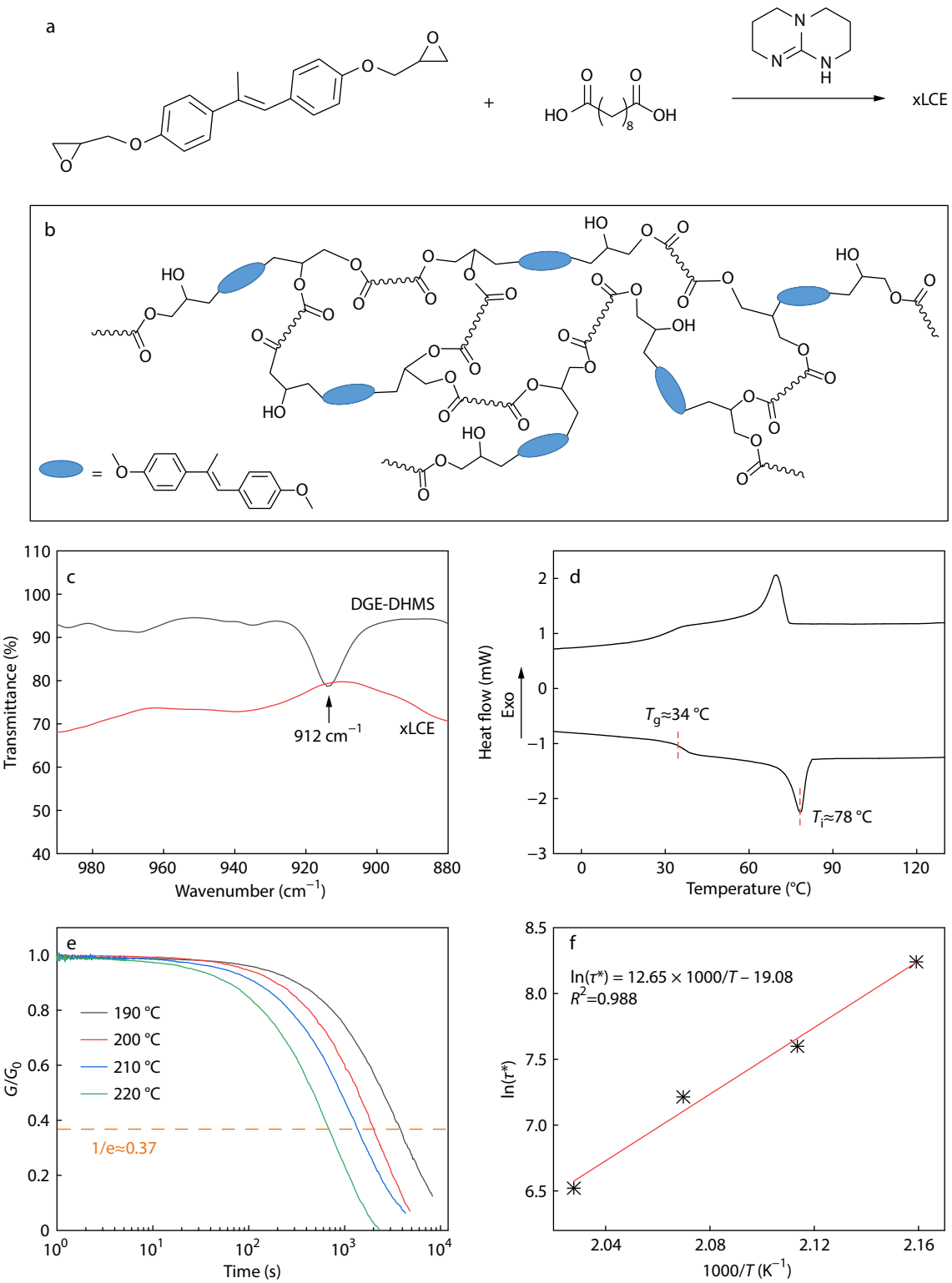

Fig. 1 Synthesis and characterizations of the polydomain xLCE: (a) the synthesis route to the polydomain xLCE; (b) The cross-linking structure of the polydomain xLCE-DHMS; (c) FTIR spectra of the monomer (DGE-DHMS) and crosslinked xLCE; (d) DCS curve of the polydomain xLCE; (e) Stress relaxation curves of the xLCE at varying temperatures, showing its intrinsic dynamic property; (f) The Arrhenius plot and corresponding fitting lines derived from stress relaxation data of the xLCE.

Shear stress relaxation experiments were measured within the linear viscoelastic region of xLCE samples between T_i and T_d until the samples had relaxed to below 1/e of the initial stress relaxation modulus. The time required for this relaxation is defined as relaxation time τ^*. As shown in Fig. 1(e), the higher the temperature, the faster the stress relaxation for the

https://doi.org/10.1007/s10118-024-3192-7

samples, and the shorter the relaxation time τ^*, indicating the activation of transesterifications at high temperatures and the rearrangement of the xLCE network topology. Relaxation times τ^* follows an Arrhenius law at temperatures above T_v. Fig. 1(f) indicated the Arrhenius plot and corresponding fitting lines derived from stress relaxation data of the xLCE. The T_v value of the samples were determined using the Maxwell equation according to the method previously reported.[33] Therefore, the T_v value of the xLCE was calculated to be 108 °C. Moreover, the mechanical properties of the xLCE were characterized based on stress-strain tests (Fig. S6 in ESI).

In this study, various locked shapes of one single monodomain xLCE were modulated by controlling the cooling rates. Water and silicone oil were employed as the mediums, and elongation strains of monodomain xLCE samples with reversible elongation mode were investigated. Specifically, the monodomain xLCE samples were heated to 100 °C (above the T_i), resulting in the xLCEs being at their shortest length. These samples were then quickly transferred into water or silicone oil with various initial temperatures. Their corresponding equilibrium elongation strains were measured when the mediums (water or silicone oil) cooled to room temperature, demonstrating different cooling rates. The calculation of the elongation strain can be found in ESI. The results are presented in Fig. 2(a). Regardless of water or oil, the elongation strains of the xLCE show a positive correlation with temperatures. In other words, the higher the initial temperature of the mediums, the higher the elongation strain of the xLCE sample. The reason is that these elongation strains depended on the natural cooling rates of the two mediums. Since the cooling rate of water is faster than that of silicone oil, the monodomain xLCE cooled in water shows a smaller elongation strain compared to the one cooled in silicone oil.

Different cooling rates were established to facilitate the subsequent analysis of the identical xLCE sample. We tested the temperature curves over time from 100 °C to room temperature under water and silicone oil mediums (Fig. S7 in ESI). The curves showed that their cooling rates are not constant values. Therefore, three cooling rates (fast, medium, and slow cooling rate) were applied by utilizing the water with initial temperatures of 100, 60 and 0 °C, respectively. As described in Fig. 2(b), diverse locked elongation shapes of one xLCE with three different cooling rates were recorded at room temperature, namely mono-fast, mono-medium, and mono-slow, respectively. Correlating with Fig. 2(a), it was evident that the elongation strains of the xLCE subjected to fast, medium, and slow cooling were 4%, 49%, and 98%, respectively. Furthermore, the locked shape upon the same cooling rate would be affected by the thickness of the sample. As shown in Fig. S8 (in ESI), the thicker sample (0.33-mm-thickness) exhibits a larger elongation strain compared to the thinner sample (0.12-mm-thickness) under a medium cooling rate.

Moreover, the liquid crystal-isotropic transition of the xLCE is a first-order phase transition and is temperature-dependent as mentioned above. When the actuated shape underwent fast cooling from an elevated temperature, the phase transition would be delayed, resulting in the xLCE remaining in an isotropic phase to lock the actuated contraction deformation, which was demonstrated by the mono-fast sample. Conversely, a slow cooling rate enabled nearly full recovery of

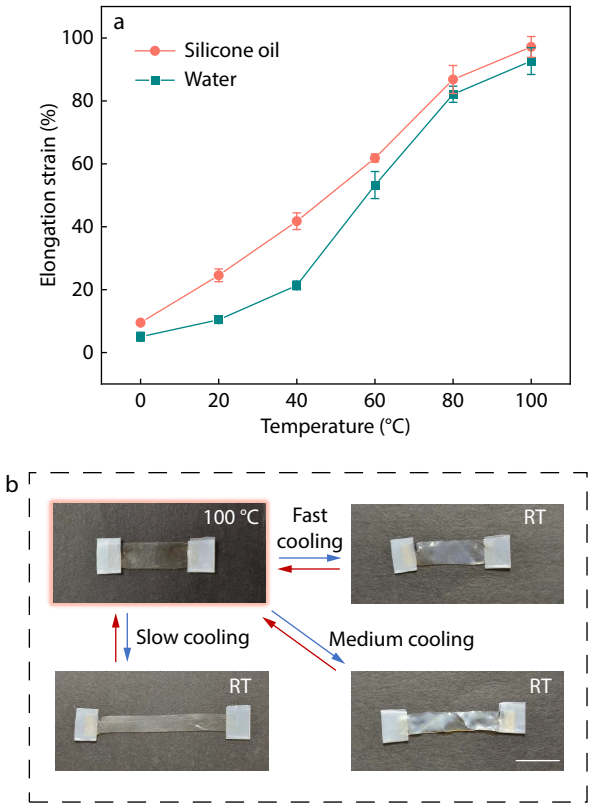

Fig. 2 Various locked shapes of one monodomain xLCE with reversible elongation mode were modulated by controlling the cooling rates: (a) Relationship of the elongation strain of the xLCE and the initial temperature based on two cooling mediums (silicone oil and water); (b) Schematic illustration of diverse locked elongation shapes of the xLCE with three different cooling rates, namely mono-fast, mono-medium, and mono-slow, respectively. Scale bar: 10 mm

the original elongation shape, while the intermediate shape was obtained by using a medium cooling rate, demonstrated by mono-slow and mono-medium samples. The locked shapes were stable at room temperature since the T_g of the epoxy xLCE was higher than room temperature.

The alignment of the polydomain, mono-fast, mono-medium, and mono-slow xLCEs was confirmed via two-dimensional (2D) X-ray diffraction (XRD) tests (Fig. 3a). The XRD image of the polydomain xLCE showed two uniform rings, suggesting no orientational bias in either wide-angle (nematic) or small-angle (smectic) scattering. The XRD patterns of the monodomain xLCEs subjected to different cooling rates indicated that slower cooling rates corresponded to more pronounced diffraction ring splitting and enhanced orientation.

Fig. 3(b) shows the Azimuthal intensity scan of XRD patterns from the abovementioned samples. It was obvious that diffraction intensity peaks just appeared in the monodomain xLCEs. Similarly, the slower the cooling rate, the stronger the diffraction intensity. The orientational (nematic) order parameters of mono-fast, mono-medium, and mono-slow xLCEs were calculated to be 0.28, 0.68 and 0.80, respectively (the details can be found in the ESI). In conjunction with the previously mentioned elongation strain data, it was observed that the orientation degrees and the elongation strains of xLCEs

https://doi.org/10.1007/s10118-024-3192-7

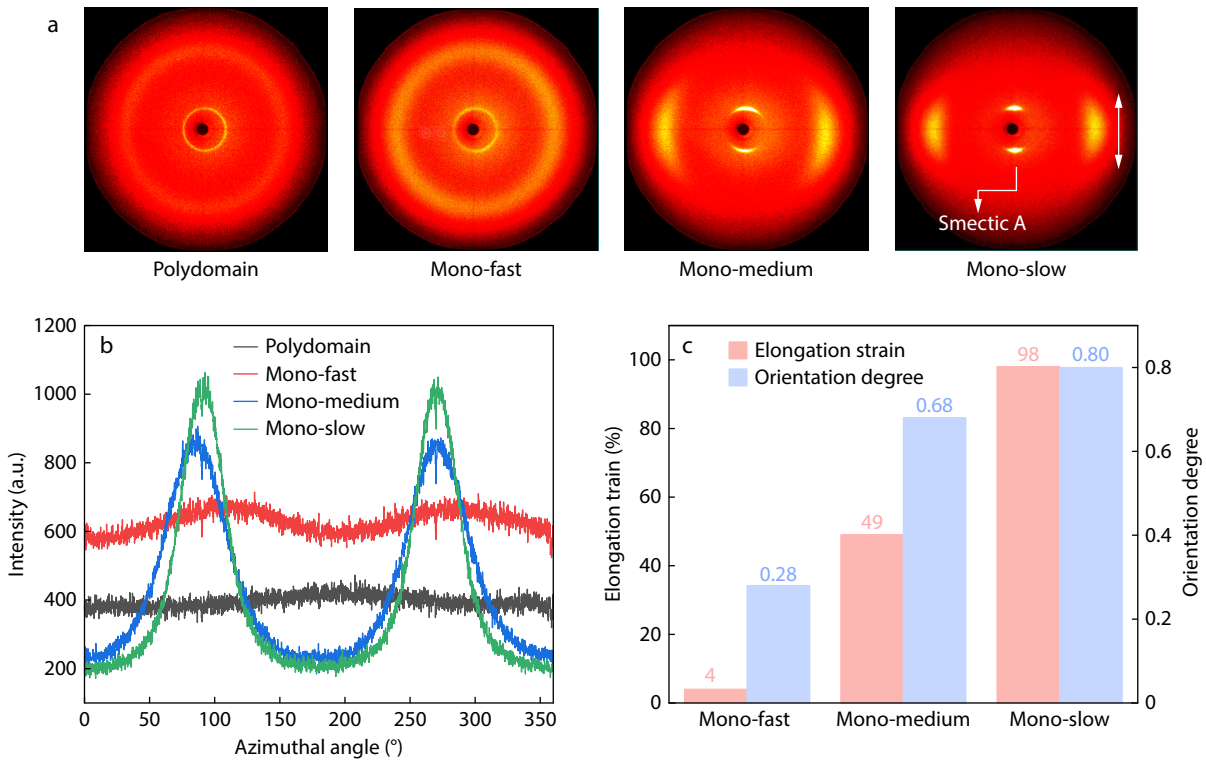

Fig. 3 Analysis of the alignment of the polydomain, mono-fast, mono-medium, and mono-slow xLCEs: (a) X-ray diffraction images of xLCEs (the arrow denotes the aligning direction); (b) Azimuthal intensity scan of xLCEs; (c) Elongation strains and orientation degrees of xLCEs.

increased as the cooling rates decreased (Fig. 3c).

To further demonstrate the influence of the cooling rate on the shape-locking of one single monodomain sample, we selected an xLCE with bending actuation mode as an example. Fig. 4(a) displays various locking bending deformations at room temperature *via* different cooling rates. It was observed that faster cooling rates resulted in smaller bending degrees, whereas slower cooling rates led to larger bending degrees. This experiment reaffirmed that controlling the temperature of the medium can indeed regulate the degree of anisotropy of LC mesogens, and subsequently modulate the shape changes of the xLCE.

As mentioned above, this xLCE system was capable of reprogramming with diverse reversible actuation modes owing to its intrinsic dynamic covalent bonds. Specifically, the xLCE with elongation actuation mode can be readily re-aligned by deforming the sample (*e.g.*, spiraling) and fixing the new orientation of mesogens at elevated temperatures (Fig. 4b). Therefore, the same xLCE with new spiraling actuation mode was obtained. Similarly, spiral shapes can be controlled by cooling rates. Faster cooling rates yielded smaller spiraling degrees and fewer spiral cycles, while slower ones yielded larger spiraling degrees and more spiral cycles.

Furthermore, beyond the previously discussed cooling methods, it was discovered that copper plates with different thicknesses can serve as the medium with distinct cooling rates. This enabled the modulation of elongation deformations in an identical monodomain xLCE with reversible elongation motion mode. Specifically, a monodomain xLCE film was fabricated and fixed onto a 0.01-mm-thick copper plate using a PTFE tape (located in the center of the film). A polyimide strip was applied to both ends of the film to create an arc. The copper plate was placed on a heating stage at 100 °C (Fig. 4c-i). Upon reaching the minimum length of the xLCE film, the heating source was removed and the copper plate was allowed to cool to room temperature naturally. The elongation length of the xLCE film controlled by a 0.01-mm-thick copper plate and the corresponding arching height of the polyimide strip were shown in Fig. 4(c-ii). Subsequently, varying the thickness of the copper plate (0.05 mm, 0.1 mm, 0.5 mm, 1 mm, 2 mm, 3 mm) to repeat the above process, it was evident that with an increase in the thickness of the copper plate, there was a corresponding decrease in the cooling rate, resulting in a prolonged elongation of the xLCE and a reduction in the arching height of the strip at room temperature, as indicated in Figs. 4(c-ii)–4(c-viii). Moreover, corresponding elongation strains of the xLCE subjected to different cooling rates can be calculated. As shown in Fig. S9 (in ESI), thicker copper plates functioned as the mediums with slower cooling rates, resulting in higher elongation strains of the xLCE.

CONCLUSIONS

In conclusion, we propose a strategy to regulate actuation modes and locked shapes of xLCEs by combining dynamic covalent bonds with cooling-rate-mediated control. The actuation modes, including elongating, bending, and spiraling, were programmed and reprogrammed *via* dynamic exchange reactions. Based on this approach, the proposed cooling-rate-mediated methods, which involve controlling the types of mediums (water, oil, and copper plates) and their initial temperatures, have effectively yielded diverse locked shapes of xLCEs. These findings underscore the potential applications of xLCEs in multi-

https://doi.org/10.1007/s10118-024-3192-7

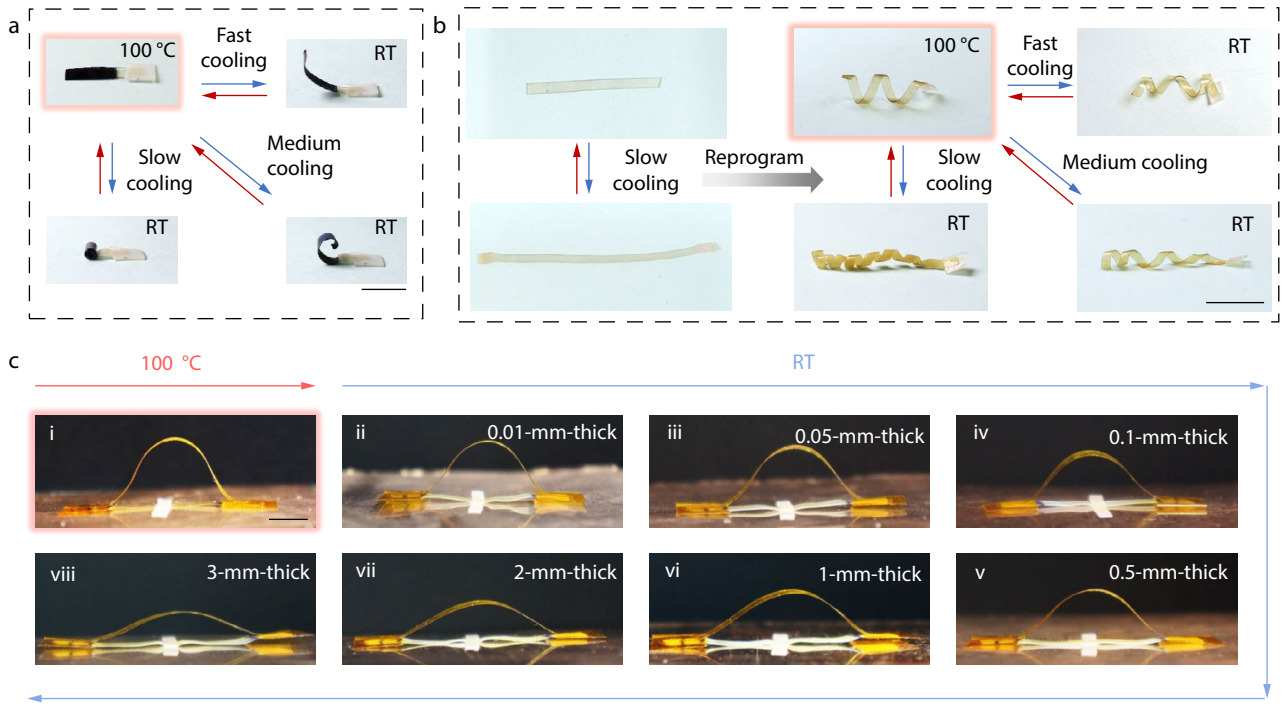

Fig. 4 Multiple locked shapes of xLCEs with different actuation modes were regulated by controlling the cooling rates *via* water or copper plates cooling mediums: (a) Schematic illustration of varying locked bending shapes of the xLCE with three different cooling rates. Scale bar: 10 mm; (b) Schematic illustration of reprogramming the elongation actuation mode to spiraling actuation mode, and corresponding cooling-rate-mediated locked spiral shapes. Scale bar: 10 mm; (c) Schematic illustration of the modulation of elongation deformations by copper plates with different thicknesses. Scale bar: 5 mm.

modal structures, thereby expanding their versatility and utility in various fields. Meanwhile, the orientation degrees and the elongation strains of xLCEs increased as the cooling rates decreased. The obtained locked shapes were robust at room temperature ranges. This strategy offers a straightforward approach to enhance the deformation diversity of xLCEs while eliminating the requirement for continuous external stimuli or energy input to sustain shape morphing. the combination of dynamic covalent bonds and cooling-rate-mediated control holds promise in enabling xLCE systems with enhanced programmability, controllability of motions, as well as increased adaptability. The advantages of this strategy cater to a diverse array of applications such as artificial muscles, wearables, and bionic robots.

Conflict of Interests

The authors declare no interest conflict.

Electronic Supplementary Information

Electronic supplementary information (ESI) is available free of charge in the online version of this article at http://doi.org/10.1007/s10118-024-3192-7.

Data Availability Statement

The data that support the findings of this study are available from the corresponding author upon reasonable request. The author's contact information: lianghuan@mail.tsinghua.edu.cn.

ACKNOWLEDGMENTS

This work was financially supported by the National Natural Science Foundation of China (No. 22375114).

REFERENCES

1 Herbert, K. M.; Fowler, H. E.; McCracken, J. M.; Schlafmann, K. R.; Koch, J. A.; White, T. J. Synthesis and alignment of liquid crystalline elastomers. *Nat. Rev. Mater.* **2021**, *7*, 23–38.
2 Zhang, C.; Fei, G.; Lu, X.; Xia, H.; Zhao, Y. Liquid crystal elastomer artificial tendrils with asymmetric core-sheath structure showing evolutionary biomimetic locomotion. *Adv. Mater.* **2024**, *36*, 2307210.
3 Kim, S. U.; Lee, Y. J.; Liu, J.; Kim, D. S.; Wang, H.; Yang, S. Broadband and pixelated camouflage in inflating chiral nematic liquid crystalline elastomers. *Nat. Mater.* **2022**, *21*, 41–46.
4 Wang, M.; Song, Y.; Bisoyi, H. K.; Yang, J. F.; Liu, L.; Yang, H.; Li, Q. A liquid crystal elastomer-based unprecedented two-way shape-memory aerogel. *Adv. Sci.* **2021**, *8*, 2102674.
5 Chen, M.; Gao, M.; Bai, L.; Zheng, H.; Qi, H. J.; Zhou, K. Recent advances in 4D printing of liquid crystal elastomers. *Adv. Mater.* **2023**, *35*, 2209566.
6 Yin, L.; Han, L.; Ge, F.; Tong, X.; Zhang, W.; Soldera, A.; Zhao, Y. A novel side-chain liquid crystal elastomer exhibiting anomalous reversible shape change. *Angew. Chem. Int. Ed.* **2020**, *59*, 15129–15134.
7 Schlafmann, K. R.; White, T. J. Retention and deformation of the

blue phases in liquid crystalline elastomers. *Nat. Commun.* **2021**, *12*, 4916.
8 Huang, X.; Pang, X.; Qin, L.; Yu, Y. Photodeformable main-chain crosslinked liquid crystal polymer fiber actuators at room temperature. *Acta Polymerica Sinica* (in Chinese) **2022**, *53*, 1324–1331.
9 Xiao, Y. Y.; Jiang, Z. C.; Hou, J. B.; Zhao, Y. Desynchronized liquid crystalline network actuators with deformation reversal capability. *Nat. Commun.* **2021**, *12*, 624.
10 Song, C.; Zou, B.; Cui, Z.; Liang, Z.; Ju, J. Thermomechanically triggered reversible multi-transformability of a single material system by energy swapping and shape memory effects. *Adv. Funct. Mater.* **2021**, *31*, 2101395.
11 Chen, G.; Jin, B.; Shi, Y.; Zhao, Q.; Shen, Y.; Xie, T. Rapidly and repeatedly reprogrammable liquid crystalline elastomer via a shape memory mechanism. *Adv. Mater.* **2022**, *34*, 2201679.
12 Zhang, C.; Chen, G.; Zhang, K.; Jin, B.; Zhao, Q.; Xie, T. Repeatedly programmable liquid crystal dielectric elastomer with multimodal actuation. *Adv. Mater.* **2024**, *36*, 2313078.
13 Chen, Q.; Li, W.; Wei, Y.; Ji, Y. Reprogrammable 3D liquid-crystalline actuators with precisely controllable stepwise actuation. *Adv. Intell. Syst.* **2021**, *3*, 2000249.
14 Qiu, W.; He, X.; Fang, Z.; Wang, Y.; Dong, K.; Zhang, G.; Xu, X.; Ge, Q.; Xiong, Y. Shape-tunable 4D printing of LCEs *via* cooling rate modulation: stimulus-free locking of actuated state at room temperature. *ACS Appl. Mater. Interfaces* **2023**, *15*, 47509–47519.
15 Roach, D. J.; Sun, X.; Peng, X.; Demoly, F.; Zhou, K.; Qi, H. J. 4D printed multifunctional composites with cooling-rate mediated tunable shape morphing. *Adv. Funct. Mater.* **2022**, *32*, 2203236.
16 Javed, M.; Corazao, T.; Saed, M. O.; Ambulo, C. P.; Li, Y.; Kessler, M. R.; Ware, T. H. Programmable shape change in semicrystalline liquid crystal elastomers. *ACS Appl. Mater. Interfaces* **2022**, *14*, 35087–35096.
17 Traugutt, N. A.; Volpe, R. H.; Bollinger, M. S.; Saed, M. O.; Torbati, A. H.; Yu, K.; Dadivanyan, N.; Yakacki, C. M. Liquid-crystal order during synthesis affects main-chain liquid-crystal elastomer behavior. *Soft Matter* **2017**, *13*, 7013–7025.
18 Ohzono, T.; Saed, M. O.; Terentjev, E. M. Enhanced dynamic adhesion in nematic liquid crystal elastomers. *Adv. Mater.* **2019**, *31*, 1902642.
19 Ma, J.; Yang, Y.; Valenzuela, C.; Zhang, X.; Wang, L.; Feng, W. Mechanochromic, shape-programmable and self-healable cholesteric liquid crystal elastomers enabled by dynamic covalent boronic ester bonds. *Angew. Chem. Int. Ed.* **2022**, *61*, e202116219.
20 Davidson, E. C.; Kotikian, A.; Li, S.; Aizenberg, J.; Lewis, J. A. 3D printable and reconfigurable liquid crystal elastomers with light-induced shape memory *via* dynamic bond exchange. *Adv. Mater.* **2020**, *32*, 1905682.
21 Hebner, T. S.; Podgórski, M.; Mavila, S.; White, T. J.; Bowman, C. N. Shape permanence in diarylethene-functionalized liquid-crystal elastomers facilitated by thiol-anhydride dynamic chemistry. *Angew. Chem. Int. Ed.* **2022**, *61*, e202116522.
22 Zhang, V.; Kang, B.; Accardo, J. V.; Kalow, J. A. Structure-reactivity-property relationships in covalent adaptable networks. *J. Am. Chem. Soc.* **2022**, *144*, 22358–22377.
23 Zhang, Z.; Lei, D.; Zhang, C.; Wang, Z.; Jin, Y.; Zhang, W.; Liu, X.; Sun, J. Strong and tough supramolecular covalent adaptable networks with room-temperature closed-loop recyclability. *Adv. Mater.* **2023**, *35*, 2208619.
24 Cui, C.; An, L.; Zhang, Z.; Ji, M.; Chen, K.; Yang, Y.; Su, Q.; Wang, F.; Cheng, Y.; Zhang, Y. Reconfigurable 4D printing of reprocessable and mechanically strong polythiourethane covalent adaptable networks. *Adv. Funct. Mater.* **2022**, *32*, 2203720.
25 Wang, Y.; Yang, L.; Zhang, L.; Huang, H.; Qian, B.; Gu, S.; You, Z. Solvent-free synthesis of self-healable and recyclable crosslinked polyurethane based on dynamic oxime-urethane bonds. *Chinese J. Polym. Sci.* **2023**, *41*, 1725–1732.
26 Ye, J.; Zu, Z.; Lin, Z.; Xiang, H.; Zhang, M. Intrinsic self-healing polysiloxane materials: from single dynamic crosslinked network to multiple dynamic crosslinked networks. *Acta Polymerica Sinica* (in Chinese) **2023**, *54*, 1028–1054.
27 Xu, H.; Zhang, Y.; Wang, H.; Wu, J. R. Unraveling the heterogeneity of epoxy-amine networks by introducing dynamic covalent bonds. *Chinese J. Polym. Sci.* **2023**, *41*, 926–932.
28 Ma, J.; Porath, L. E.; Haque, M. F.; Sett, S.; Rabbi, K. F.; Nam, S.; Miljkovic, N.; Evans, C. M. Ultra-thin self-healing vitrimer coatings for durable hydrophobicity. *Nat. Commun.* **2021**, *12*, 5210.
29 Debsharma, T.; Amfilochiou, V.; Wróblewska, A. A.; De Baere, I.; Van Paepegem, W.; Du Prez, F. E. Fast dynamic siloxane exchange mechanism for reshapable vitrimer composites. *J. Am. Chem. Soc.* **2022**, *144*, 12280–12289.
30 Santiago, D.; Guzmán, D.; Padilla, J.; Verdugo, P.; De la Flor, S.; Serra, À. Recyclable and reprocessable epoxy vitrimer adhesives. *ACS Appl. Polym. Mater.* **2023**, *5*, 2006–2015.
31 Giamberjni, M.; Amendola, E.; Carfagna, C. Liquid crystalline epoxy thermosets. *Mol. Cryst. Liq. Cryst. Sci. Technol. Sect. A-Mol. Cryst. Liq. Cryst.* **1995**, *266*, 9–22.
32 Pei, Z.; Yang, Y.; Chen, Q.; Terentjev, E. M.; Wei, Y.; Ji, Y. Mouldable liquid-crystalline elastomer actuators with exchangeable covalent bonds. *Nat. Mater.* **2014**, *13*, 36–41.
33 Kamarulzaman, S.; Png, Z. M.; Lim, E. Q.; Lim, I. Z. S.; Li, Z.; Goh, S. S. Covalent adaptable networks from renewable resources: crosslinked polymers for a sustainable future. *Chem* **2023**, *9*, 2771–2816.

https://doi.org/10.1007/s10118-024-3192-7